The EuroBiotech Journal
RESEARCH ARTICLE
Medical Biotechnology

Cell contractile force measured using a deformable hollow capsule

Julia Ho Yee Ting, Donald K Martin*

Abstract

There are several possible ways to measure the contraction of cells *in vitro*. Here, we report measurements of the contractile properties of 3T3-L1 cells grown to confluence on 3D hollow capsules. The capsules were fabricated using the layer-by-layer polyelectrolyte deposition technique on a polymer core. After the polyelectrolyte film was completed, the core was dissolved to leave the hollow capsule. The contractile force of the cells was determined from the deformation in the capsule size induced by interruption of the actin cytoskeleton of the cells that adhered to the outer surface of the hollow capsules, using prior measurements of the elastic modulus of the capsule. From the measurements of the compressive modulus for the capsules (of 6.52 μN), those capsule deformations indicate that the forskolin relaxed the layer of cells by 19.6 μN and the cytochalasin-D relaxed the layer of cells by 45.6 μN. The density of cells in the layer indicated that the force associated with the forskolin-induced relaxation of a single cell is 3.2 nN and the force associated with the cytochalasin-D-induced relaxation of a single cell is 7.5 nN. The mechanism of action of forskolin through second messenger pathways to disrupt the assembly of actin stress fibres also explains its reduced effect on cell contraction compared to that for cytochalasin-D, which is a compound that directly inhibits the polymerization of F-actin filaments.

Keywords: 3T3-L1 cell, contractile force, hollow capsule, deformation

Introduction

There are several possible ways to measure the contraction of cells *in vitro*. The simplest would be to measure the projected surface area of the cell over time, but cell contraction could not be distinguished from cell detachment or shrinkage and the force of the contraction could not be quantified. To provide quantifiable measurements of contractile forces, a better approach is to allow cells to adhere to a substrate of known viscosity that then transduces the force applied by the cell from measurements of the substrate deformation. Harris et al (1) pioneered the use of a 2D silicone substrate to measure the contractile forces during cell locomotion. We have previously used that approach to investigate the role of protein kinase-A pathways to control the contractility of retinal pericytes (2). More sophisticated two-dimensional (2D) substrates may be utilized to measure contractile force, such as substrates that incorporate micro-pillars (3) or microcantilevers (4). Although such 2D substrates provide important information on contractile forces, cells are not in their native morphology and hence those measurements may not reflect their natural in vivo contractile force. For example, it has been shown that bovine retinal pericytes and aortic endothelial cells grown in three-dimensional (3D) systems have very different morphologies to when these are grown in 2D on glass coverslips (5). The use of collagen as a matrix for 3D contraction assays has been known since the 1970s (6). Cells are embedded or seeded into the collagen gel and the changes in size of the gel can be easily monitored over time to deduce the contraction of vascular cells (5). However, collagen and other substrates such as matrigel usually provide a matrix for cell inclusion but not a 3D structure for cell growth that contains a lumen.

Univ. Grenoble Alpes, CNRS, UMR 5525, VetAgro Sup, Grenoble INP, TIMC-SyNaBi, 38000 Grenoble, France

***Corresponding author:**
Prof D.K. Martin (don.martin@univ-grenoble-alpes.fr)

DOI: 10.2478/ebtj-2022-0009

It would be ideal to assay cell contraction using a 3D format that contains a lumen, particularly for example to measure the contractile properties of vascular cells. An artificial blood vessel provides such an alternative and it has been shown that physiological mechanical properties such as stress, strain (7), tensile strength (8), and compression (9) can be achieved. For example, Amiel et al were able to produce engineered vessels with a diameter of 3-4mm that supported the growth of viable HUVEC cells (10). Takei et al constructed collagen tubules consisted of two types of vascular cells (endothelial and smooth muscle cells) that could withstand physiological levels of shear stress (11). Although those studies shows advances towards artificial capillaries, the engineering processes involved are often very complex and, more importantly, it has not been shown that the luminal size of these systems are tunable by cell contraction and relaxation.

Advances in nano- and biotechnology research have gained considerable attention in the recent years and have shed light on potential new material and techniques that may be useful for tissue engineering. In particular, Decher's description of nanostructured thin films composed of layered polyelectrolytes (12) has stimulated a great deal of research published using such polyelectrolyte thin films. These films can be deposited/coated on almost any surface, including bacterial and red blood cells (13), plastic, glass and latex, using a simple layer-by-layer (LbL) assembly technique, which also means that it is easy to tune the thickness and strength of the structure by varying the number of polyelectrolyte layers deposited. An interesting aspect of polyelectrolyte thin films is that the terminating (basal lamina side) charge of the thin films can modulate the actin distribution in cells (14) and cell proliferation (15). It is also known that capsules made using polyelectrolyte thin films are elastic, relatively stable, and able to withstand very acidic and alkaline environments. We have shown that HEK293 cells (kidney epithelial cells from human embryo) and 3T3-L1 cells (fibroblasts from mouse embryo) adhere and grow onto polyelectrolyte films constructed using anionic poly(sodium 4-styrenesulphonate) (PSS) and cationic poly(allylamine hydrochloride) (PAH) (16). We have also shown that PAH/PSS hollow capsules constructed using a melamine formaldehyde core were able to retain a spherical shape and support the adsorption of a lipid bilayer into which we incorporated ion-transporting proteins (17). Those capsules had a diameter of 6.5 μm and were suitable for patch-clamp electrophysiology, but were too small for the purposes of this current manuscript to measure cell contractile forces.

Here, we have designed larger diameter self-supporting hollow capsules by using the LbL formation of a PAH/PSS film over a biopolymer core. We have previously shown that such a PAH/PSS/biopolymer system results in the formation of an interpenetrating polymer that is around 280 nm in thickness, is self-supporting, remains permeable, and retains the surface charges of the polyelectrolytes to facilitate the adsorption of a lipid bilayer (18). Here, we utilized the concept of this interpenetrating polymer to form hollow self-supporting capsules of a diameter around 2 mm, and then grew a confluent layer of 3T3-L1 cells on the hollow capsules. Two F-actin disrupting compounds, forskolin and cytochalasin-D, were used in separate experiments to relax the cells by removing the cytoskeletal contractile stress exerted by the cells on the capsules. The contractile force of the cells was determined from the change in the capsule size induced by disruption of the actin cytoskeleton of the cells that adhered to the outer surface of the hollow capsules. Our measurements of the compressive modulus of the capsules without cells allowed us to quantify the magnitude of the contractile force that was associated with the change in capsule size.

Materials and Methods

Preparation of the hollow capsules for cell growth

The material for the spherical cores used for templating the hollow capsules was prepared from chitosan (2% w/v) that was dissolved in 2% acetic acid (2% w/v), left overnight at room temperature and then diluted to 1.5% chitosan with ethanol. The spherical cores were made by dropping small volumes of the chitosan (1.5% diluted) solution through a 27G needle into a warm bath of 5M NaOH/ethanol (1:1 ratio) using an syringe pump. The change in pH in the warm bath solution stimulated the cross-linking of the chitosan to form polymer spheres of a diameter approximately 2mm.

A standard layer-by-layer (LbL) technique was used to form a polyelectrolyte multilayered film on the chitosan spherical cores by alternately adsorbing poly(allylamine hydrochloride) (PAH) and then poly(sodium styrene sulfonate) (PSS) then at 1mg/mL in 0.5M NaCl onto the surface of the chitosan cores. With the chitosan as the core material, it was important to commence the LbL procedure with PAH. The LbL technique was used to form a film of 7 to 9 layers of PAH/PSS. Then, the chitosan spherical core was dissolved by washing the coated spheres in acetic acid (2% w/v) and then incubating the washed spheres overnight in acetic acid (2% w/v) overnight to form hollow capsules. These hollow capsules were then washed with 70% ethanol three times in preparation for cell culture, then with cell culture medium three to four times to remove all traces of ethanol.

Compressive stiffness of the hollow capsules

The compressive stiffness was measured by compressing a capsule and measuring its deformation. For these measurements, the capsules were immersed either in HEPES-buffered saline or in pure water (MilliQ). The mechanical stress to compress the capsule was applied by a piston connected to a micro-manipulator to control its position. The capsules were contained within a cuvette that was mounted on an electronic balance (accurate to 2 mg) that measured the force applied to the capsules by the piston. The force was calculated from the recording of the mass by the electronic balance. The deformation of the capsules was measured from optical sections captured by a digital camera (DCM300, Hangzhou Huaxin IC Technology Inc) mounted on an ophthalmological slit-lamp biomicroscope (Zeiss). The

cross-sectional area of these optical sections was measured from the digital images using Image Pro Plus 5.0.

Cell culture

Cultures of mouse embryonic adipose-like fibroblast cells 3T3-L1 were maintained in 10% FBS in DMEM (Invitrogen 21063-045) and incubated at 37°C, in a 5% CO_2 atmosphere. Cells were passaged using Trypsin-EDTA (Sigma T4299) for 5 minutes.

Measurement of cell contraction force

Hollow capsules were added to the media in 24-well plates, and then 3T3-L1 cells were seeded into the wells (100,000 cells/well). The cells were allowed to grow to confluence on the capsules. Then the capsules-plus-cells were transferred to a 35mm individual dish that had glass beads glued to the bottom. The purpose of the glass beads was to confine the capsules-plus-cells to avoid their movement during the following measurements. First, the projected surface area of the capsules-plus-cells was measured from images captured using a digital camera (DCM300, Hangzhou Huaxin IC Technology Inc) attached the observation microscope. The surface area was measured using Image Pro Plus 5.0. Then, either forskolin (10 μM) or cytochalasin-D (10 μM) was added to the media in the 35mm dish and left to incubate for 40 minutes. Then, the surface area of the same capsules-plus-cells was measured from images captured using a digital camera (DCM300, Hangzhou Huaxin IC Technology Inc) attached the observation microscope. The surface area was measured using Image Pro Plus 5.0. The forskolin or cytochalasin-D disrupted the actin cytoskeleton and hence reduced the contractile force exerted by the cells on the capsules. The magnitude of the reduction in contractile force was calculated from the change in the projected surface area of the capsules-plus-cells before and after adding either forskolin or cytochalasin-D. By reference to the prior measurements of the elastic moduli of the capsules the cell contraction force was determined from the deformation induced to the capsules by the cells.

Microscopy of capsules and cells

The capsules were imaged using confocal microscopy to confirm the dissolution of the chitosan cores and measure the thickness of the capsule walls. The capsules were stained with 1 mg/mL FITC-dextran (Sigma, FD10S). An Olympus FE300 Confocal Microscope with Fluoview 300 software was used to capture optical sections which were analysed using Image Pro Plus 5.0 for measurements of the capsule wall thickness.

Physical sections of the adherent cells on the capsules were imaged separately using fluorescence microscopy. The 3T3-L1 cells were seeded on the capsules as for the contraction measurements and grown to confluence, then stained with CFDA (Invitrogen, C1157), which is a long-term fluorescent indicator for live cells. The cells were then fixed with 4% paraformaldehyde. The fixed capsules, with and without cells, were first embedded in a plasma clot to form a cell block (a standard cytology method) and then physical sections made using auto tissue processors for sectioning. In separate measurements, the ultrastructure of the interaction between the capsules and the adherent cells was imaged using transmission electron microscopy (TEM).

In separate experiments with cells in 2D cultures, fluorescence microscopy was also used to confirm the disruption of the cytoskeleton by forskolin and cytochalasin-D. The 3T3-L1 cells were seeded on coverslips at a density of 50,000 cells per well of a 24-well plate, and left overnight for attachment. Cells were incubated with either 10 μM forskolin, 10μM cytochalsin-D, or HEPES-buffered saline (control) at 37°C for 20 minutes, then fixed with 4% paraformaldehyde for 20 minutes. Alexa-fluo 633 phalloidin (Invitrogen, A22284) was used to stain for F-actin after the cells were extracted with 1% Triton X-100 for 3 minutes and blocked 1% BSA 20 minutes.

Statistics

All statistical analysis was carried out with SPSS 15.0 using independent t-tests or one way ANOVA and Tukey-Kramer analysis. The results are considered significant when $p<0.05$. Least square regression was carried out using Microsoft® Excel.

Results

Characteristics of the capsules

The hollow capsules prepared from the chitosan spherical cores as template for the LbL procedure with PAH as the starting polyelectrolyte were uniform in size. The average diameter was 2.21±0.04 mm (n=9), which corresponded to an average surface area of 15.4±0.06 mm^2 (n=9). We tried an alternative LbL procedure by using PSS as the starting polyelectrolyte, but that procedure produced hollow capsules with a smaller diameter (2.05±0.04 mm, n=9) and a smaller surface area (13.30±0.05 mm2, n=9). Also, the use of PSS as the starting polyelectrolyte produced capsules that had thicker walls (Figure 1a). The micrometre range of wall thickness for these capsules is due to the interpenetrating polymer that is produced by the LbL technique used with a biopolymer (18). Since the purpose of the hollow capsules was to provide a soft deformable substrate for the assessment of the contraction of adhering cells, we decided to utilise the LbL procedure with PAH as the starting polyelectrolyte because the interpenetrating polymer produced capsules with thinner walls.

The walls of the capsules remained permeable, which was a necessary characteristic to facilitate the dissolution of the chitosan core. Figure 1b shows the fluorescence intensity measured inside capsules with walls formed either with PAH or PSS as the starting polyelectrolyte. The capsules formed using PAH as the starting polyelectrolyte were more permeable to FITC-dextran, which was a characteristic important for the dissolution of the chitosan core material.

To confirm that the chitosan core dissolved completely, the capsules were stained with FITC-dextran and imaged using confocal microscopy (Figure 2). The outer wall of the capsules is uniformly and brightly stained. For the capsules formed using

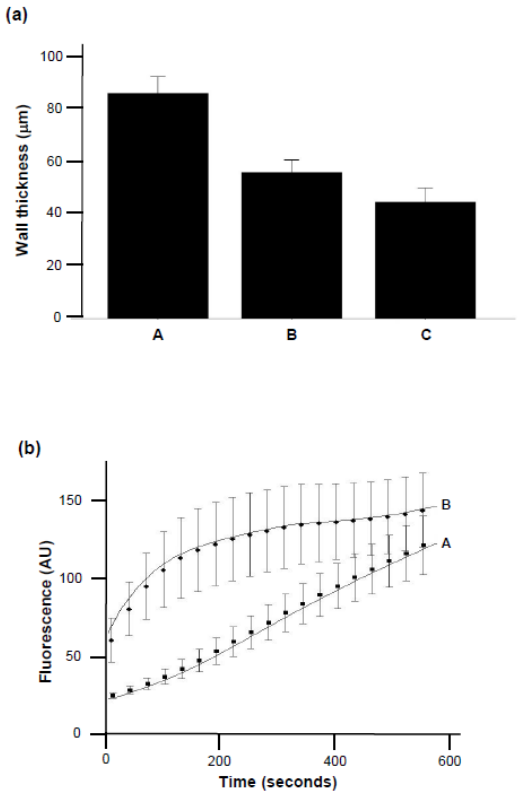

Figure 1. Characteristics of the hollow capsules. (a) The wall thickness of capsules made using (A) PSS as the sta ting polyelectrolyte, or (B,C) PAH as the starting polyelectrolyte. The histograms for the PAH-starting capsules are for (B) optical sections of the capsules, or (C) physical sections made by embedding the capsules. The error bars on each histogram represent the standard error from measurements of more than 9 capsules in each condition. (b) The permeability of the capsules to FITC-dextran measured by the increase in fluorescence of the interior of the capsules when FITC-dextran was added to the bathing solution. The fluorescence is reported as arbitrary units (AU). The curves are labelled using the same nomenclature as for wall thicknesses reported in panel (a). Thus, the permeability measurement labelled A is for capsules made using PSS as the starting polyelectrolyte, and B indicates the permeability measurements for capsules made using PAH as the starting polyelectrolyte.

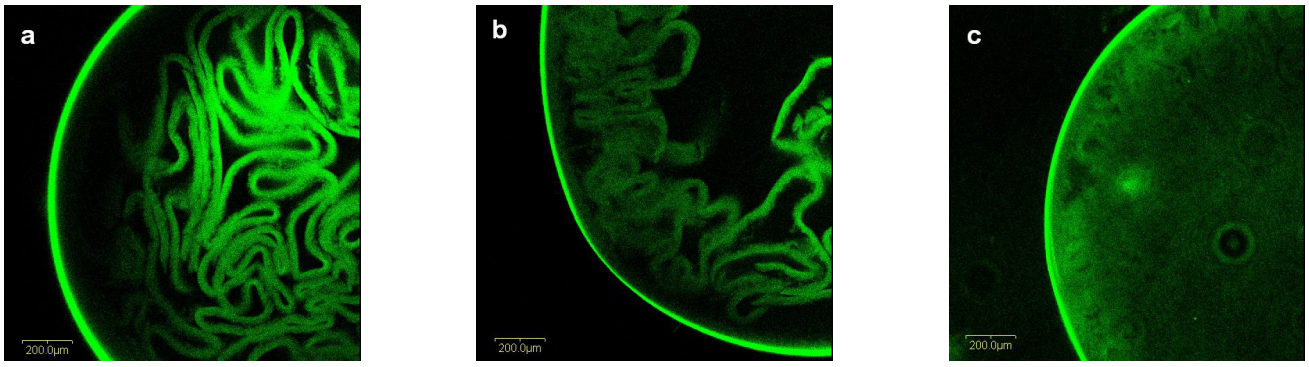

Figure 2. Confocal microscopy sections of the polyelectrolye capsules made using PAH as the starting polyelectroyte. (a) the PAH-starting capsules immersed in HEPES-buffered saline, (b) the PAHstarting capsules after washing in acetic acid (2%), and (c) the PAH-starting capsules after an overnight incubation in acetic acid (2%). The outer wall of the capsules is uniformly and brightly stained. The chitosan core remnants are imaged as coiled, slightly discontinuous and wrinkled membrane-type segments. The remnants of the chitosan core material are dissolved with an overnight incubation in acetic acid (2%).

PAH as the starting polyelectrolyte, incubation in HEPES-buffered solution showed that the interior of the capsule retained much of the chitosan core (Figure 2a). In Figure 2a the chitosan core remnants are imaged as coiled, slightly discontinuous and wrinkled membrane-type segments. Washing in acetic acid (2%) dissolved some of the chitosan remnants inside the capsules (Figure 2b). Overnight incubation in acetic acid (2%) removed all of the wrinkled membrane-type remnants of chitosan. Thus, for the rest of the experiments the capsules were produced using the LbL procedure with PAH as the starting polyelectrolyte, and the capsules were not used until after an overnight incubation in acetic acid (2% w/v).

Compressive stiffness of the hollow capsules

The stiffness of the capsules was determined by measuring the deformation of a capsule in response to a compressive force, with an apparatus mounted onto a slit-lamp biomicroscope to allow optical sections of the capsules to be photographed (Figure 3). The range of deformations did not exceed 12%. The capsules prepared with PSS as the starting polyelectrolyte were stiffer that the capsules prepared with PAH as the starting polyelectrolyte. This can be seen in Figure 4a, where the compression results are shown for the hollow capsules after the chitosan core had been removed by dissolving with acetic acid during an overnight incubation. The PSS-starting capsules required more compressive force to reach a similar level of deformation as the PAH-starting capsules. For example, to achieve a deformation of 6% the compressive force required was 120 μN for the PSS-starting capsules and 50 μM for the PAH-starting capsules. The slope of the compression/deformation measurements is interpreted as a compressive modulus for the capsules within a linear range of deformation. The PSS-starting capsules had the largest compressive modulus of 18.97±1.92 μN (n=15, R^2 of 0.841), then PAH-starting capsules measured in pure water of 9.43±1.31 μN (n=15, R^2 of 0.727), and then PAH-starting capsules measured in HEPES-buffered saline of 6.52±0.78 μN (n=15, R^2 of 0.795). We confirmed that the dissolution of the chitosan core did produce softer hollow capsules by comparing the compressive modulus measured for capsules where the chitosan core was not removed. The results shown in Figure 4b are for the compression of capsules that were incubated only in HEPES-buffered saline and hence retained the chitosan core. The compressive modulus for these core-retaining capsules was 155.57±14.14 μN (n=15, R^2 of 0.841).

For the hollow capsules, this larger compressive stiffness of the PSS-starting capsules was most likely due to their thicker walls. The PAH-starting capsules had small differences in

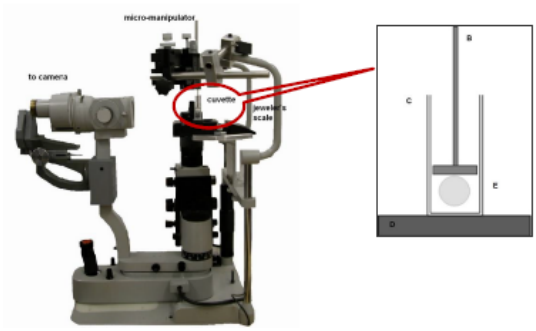

Figure 3. The modified slit-lamp biomicroscope used for the measurements. The inset illustrates the concept for the cuvette (C) that holds the capsule (E) that is compressed using the piston (B), with the force measured using the balance (D).

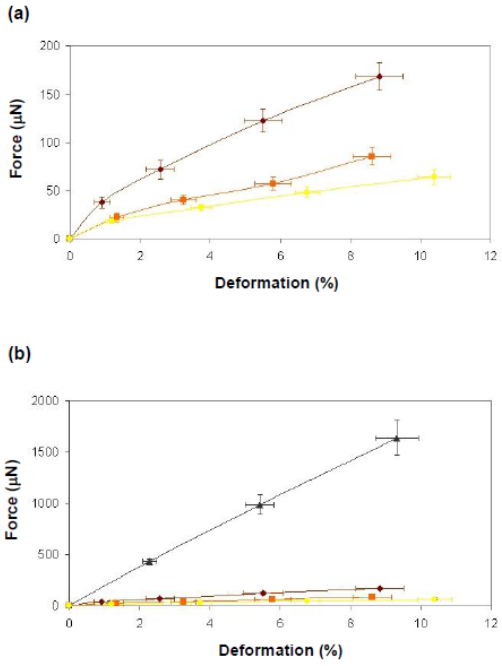

Figure 4. The compression force versus deformation for the polyelectrolye capsules. (a) graph summarising the measurements of hollow capsules after dissolving the chitosan core. The results are for PSS as the starting polyelectrolyte (◊, diamonds), PAH as the starting polyelectrolyte measured separately in water (□, squares) and in HEPES-buffered saline (o, circles). (b) the compression force versus deformation for capsules that retained their chitosan core. For these measurements the capsules were formed using PAH as the starting polyelectrolyte but were not incubated with acetic acid to dissolve the chitosan core. These PAH-starting capsules plus core were measured in water (Δ, triangles). The results from panel (a), using the same symbols and colours, are also included for comparison. The measurements are the average of 15 samples in each condition and the error bars represent the standard error.

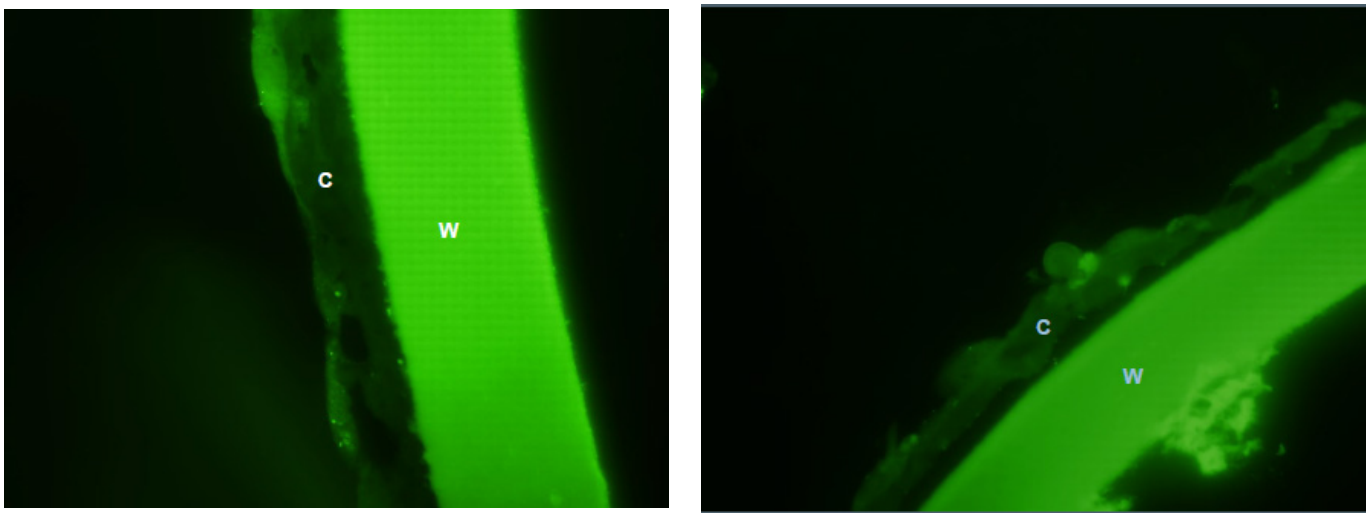

Figure 5. Fluorescence images of physical sections made from the PAH-starting capsules after the 3T3- L1 cells were allowed to grow to confluence. The 3T3-L1 cells were stained with CDFA. The panels show different sections from the same capsule, with the wall indicated with W and the 3T3-L1 cells indicated with C. Image magnification is 20x.

compressive stiffness that depended on whether they were immersed in a solution of either pure water or HEPES-buffered saline to make the measurements. The compression/deformation measurements further supported the choice of PAH-starting capsules as the better choice for the purposes of using the capsules to measure the contraction of adhering cells. This was because the PAH-starting capsules had a lower compressive modulus. The measurements of the cell contraction force were done using PAH-starting capsules in HEPES-buffered saline, which provided the most sensitive assay of contraction.

Measurement of cell contraction force

We first confirmed that the 3T3-L1 cells adhered to the capsules. The capsules were seeded with 3T3-LI cells that grew to confluence. Physical sections of the capsules with and without cells were obtained and viewed using a fluorescent microscope (Figure 5). The fluorescence imaging indicated that the 3T3-L1 cells had adhered to and grown onto the capsules. The capsules also became brightly fluorescent green, probably due to absorption of excess metabolized CFDA. We confirmed using TEM that the 3T3-LI cells had adhered to the capsules. The cells developed processes that inserted into the interpenetrating polymer wall of the capsules (Figure 6). The interpenetrating polymer wall material of the capsules appears as a discontinuous material that most likely is due to the porous hydrogel type structure of the interpenetrating polymer wall.

The contraction force applied by the cells onto the capsules was measured from the increase in surface area of the capsules after applying compounds that disrupted the F-actin cytoskeleton (Figure 6). In Figure 7 the change in projected surface area

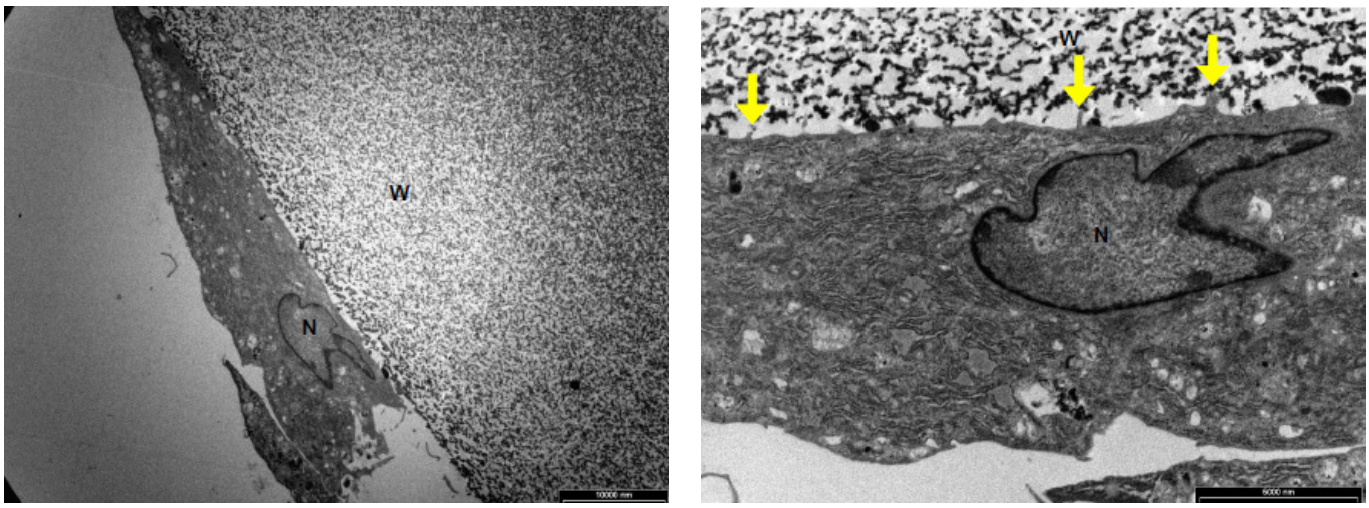

Figure 6. TEM images of the same cell on the same capsule at different magnifications. The cell nucleus is indicated with N and the capsule wall is indicated with W. The arrows indicate processs from the cell that are extending into the capsule wall. The scale bars indicate either 10,000 nm (upper panel) or 5,000 nm (lower panel).

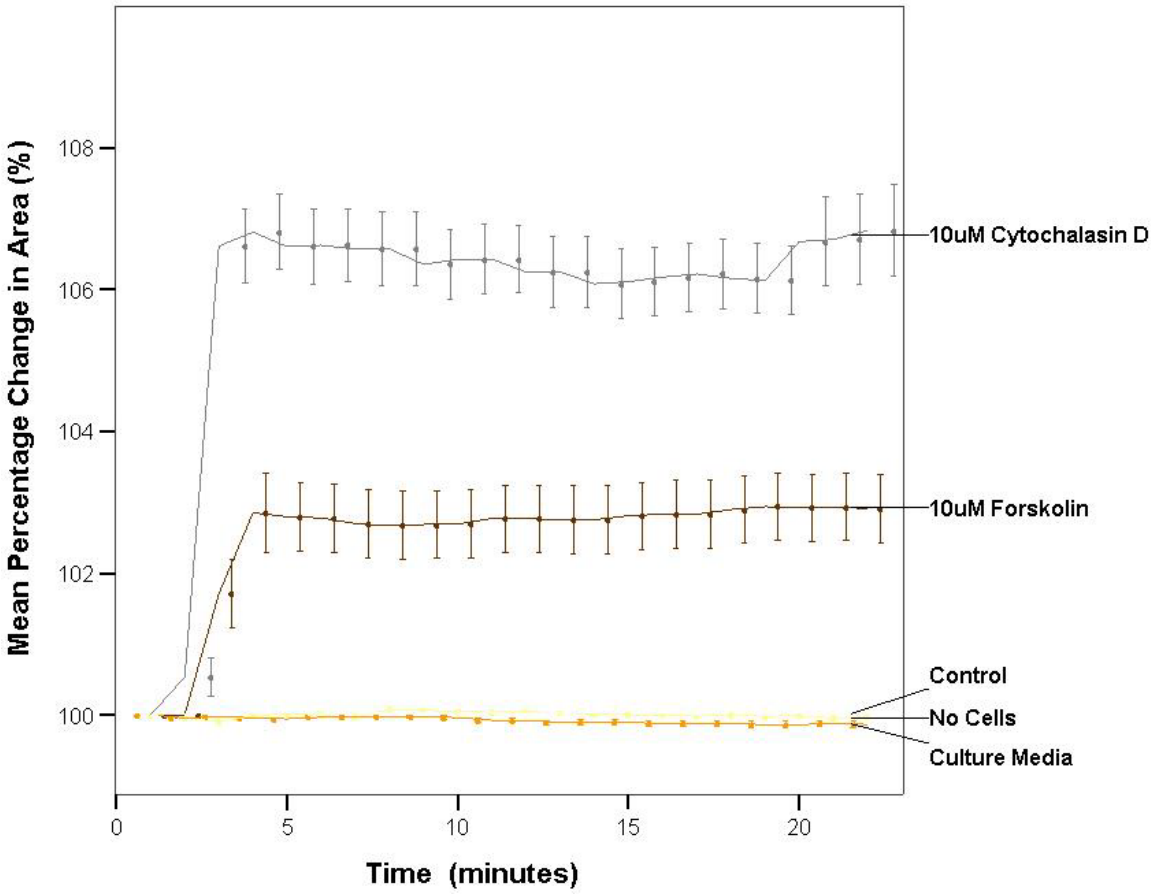

Figure 7. The change in the projected area of PAH-starting capsules that had a confluent layer of 3T3-L1 cells. The results are normalsied to the area of the capsule before addition of any compound, either culture media, forskolin (10 μM), or cytochalasin-D (10 μM). There were at least 6 independent observations made to form the average results shown by the symbols, with the bars indicating the standard error. The control conditions were either no cells grown on the capsules, or cells on the capsules exposed to culture media alone.

is normalized to the initial area of the capsules before the addition of the F-actin disrupting compounds. For both the compounds forskolin and cytochalasin-D the change in projected area (from optical sections) reached a steady-state 5 minutes after the addition of the compound to the capsules-plus-cells. After treatment with cytochalasin-D 10 μM the average increase in the area (optical sections) of the capsules was approximately 7%. After treatment with forskolin 10 μM the average increase in the area (optical sections) was approximately 3%. These measurements of increased area are due to the relaxations of the capsules following the disruption of the cytoskeleton, and also correspond to the deformation of the capsules that the contraction of the cells had exerted. From the measurements of the compressive modulus for the capsules without cells (of 6.52 μM), those deformations in the presence of the cells indicate that there was a relaxation in cell-applied force of 19.6 μN due to the action of forskolin, and a relaxation in the cell-applied force of 45.6 μN due to the action of cytochalasin-D.

The greater effect on cell contractility due to cytochalasin-D suggested that there should be a greater changed induced in the F-actin cytoskeleton by cytochalasin-D. Figure 8 shows the F-actin distribution of 3T3-L1 cells in HEPES-buffered saline and in the presence of either forskolin or cytochalasin-D. When imaged in HEPES-buffered saline the F-actin filaments in the 3T3-L1 cells are obvious and distributed throughout the cells. Addition of forskolin disrupted the distribution of F-actin filaments, but did not completely destroy the F-actin filaments. In comparison, the addition of cytochalasin-D obliterated the usual distribution of F-actin filaments. Although some F-actin filaments are still visible upon exposure to forskolin, the F-actin filaments have become segmented after exposure to cytochalasin-D.

Discussion

The purpose of this report is to describe a simple assay for cell contractility. The assay is based on the deformation of hollow polyelectrolyte capsules that have a low compressive modulus. Our results indicate that 3T3-LI cells adhere and grow to confluence on the hollow capsules. We have previously shown that PSS and PAH polyectrolyte films are not toxic to adhering 3T3-L1 cells (16). It has been reported by other scientists that PSS and PAH films are not cytotoxic to endothelial (15), osteoblast-like cells (19) as well as the 3T3-L1 cells that were used in this study (20). PSS and PAH films (21) and capsules (22, 23) have also been shown to be elastic. The simple LbL technique used to construct these polyelectrolyte films is very versatile, so

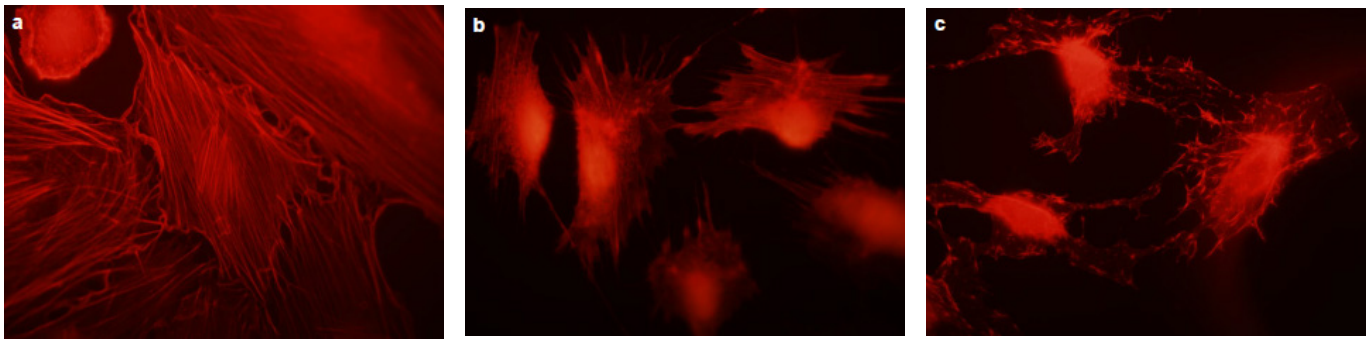

Figure 8. Fluorescence microscopy images of 3T3-L1 cells stained with AlexaFluo633 Phalloidin after fixation with paraformaldehyde. (a) cells in culture media, (b) cells after 20 minutes of exposure to forskolin (10 μM), and (c) cells after 20 minutes of exposure to cytochalasin-D (10μM). Images were made using the 100x oil immersion objective.

that almost any surface or core material may be used to construct a three dimensional and hollow scaffold.

The choice of core material can have varying effects on the properties of hollow capsules, since the core material is rarely completely eliminated and some of the solvents used to dissolve the core may crosslink polyelectrolyte chains (24). The ideal core material should be easily dissolved, but in the case where there are remnants of the core material, the level should be low, non-cytotoxic and not affect the elasticity of the capsule. Common cores used for polyelectrolyte scaffolds are melamine formaldehyde (12) and calcium carbonate (25). However, these cores are of dimension nanometres to 10 μm in diameter and hence result in the formation of capsules that are too small for cells to grow on. Alternatives for larger cores include agarose and chitosan, which are natural biopolymers derived from seaweed (agarose) and crustaceans (chitosan). These biopolymers are abundant, non-cytotoxic, biodegradable and biocompatible, which are characteristics suitable as candidates for the core material to produce larger capsules on which to grow cells for the contractility assay. The manufacturing of larger cores requires spinning of the biopolymer through a needle into the cross-linking solution. Suitable needles are 27 gauge, approximately 200 μm inside diameter, and 18 gauge, approximately 800 μm inside diameter. However, the agarose and chitosan cylindrical cores are often smaller than this because as the cylindrical cores enter into the cross-linking solution the spinning process stretches the cylinders of chitosan or agarose before solidification. The variations in the cores sizes were particularly substantial with the melt spinning of agarose because it was difficult to keep parameters constant. Agarose is a biopolymer that gels quickly at room temperature and keeping the solution in the liquid form at high temperature creates evaporation, hence the injection needs to be done quickly, preferably by hand and with a needle with larger inside diameter. This means that it is difficult to keep temperature, injection rate and agarose concentration constant, thereby making it difficult to make consistent agarose cores and the size is limited to the size of the needle.

The use of chitosan as the core material, as we report here, overcomes many of the difficulties with utilizing agarose. Changing pH is the means to control the formation of a chitosan gel. Thus the starting chitosan material can remain as a liquid at room temperature to injected at a constant rate for spinning, and at a stable concentration and with a smaller needle. The resulting chitosan spheres have diameters that are more uniform and can be made in the range from 1-2 mm. Following the LbL process for constructing the polyelectrolyte film over the core, our results indicated that the chitosan combined with the PAH/PSS to form an interpenetrating polymer. We found that the wall thickness for this interpenetrating polymer was greater when PSS was used as the starting polyelectrolyte for the LbL process. This was most likely due to the poly-anionic charge of the PSS, which would form strong ionic bonds with chitosan because it is a polymer with a positively charged pendant amino group. Although both PAH and chitosan are overall positively charged, the pKa of chitosan is approximately 6.5 and the pKa of PAH is 8.5. PAH remains strongly charged at pH 7 (19). Therefore, by coating the chitosan core material in a pH slightly above neutral with PAH as the starting polyelectrolyte our protocol produced capsules with a large diameter suitable for cell growth, small wall thickness, and low compressive modulus. By comparing the compression modulus measured in pure water to that in HBS-buffered saline, we also observed the salt softening effect in our PAH-starting capsules that has been reported for other polyelectrolyte capsules made with melamine formaldehyde as the core (22, 26).

The 3T3-L1 cells used to establish our assay method for cell contractility had abundant amounts of F-action filaments to produce their contraction. Our measurements were made in the absence of FBS, since this is reported to induce contraction of fibroblasts (27). We utilized measurements of cell relaxation in response to cytoskeleton-disrupting compounds for the following reasons. Although we could expect a reduction in the projected surface area of the capsules as the cells proliferated and contracted the PAH-starting capsules, the large size of the capsules required to support the growth of a large number of cells would have meant locating and recording the same capsule over several days. This could lead to difficulties in obtain-

ing corresponding images. The measurement of induced cell relaxation provided more controllable images that were recorded over a shorter time period.

Two F-actin disruption compounds, forskolin and cytochalasin D, were used to relax the cells by removing the cytoskeletal contractile stress exerted by the cells on the capsules. Our fluorescence microscopy indicated that forskolin and cytochalasin D produced different effects on the actin cytoskeleton of the 3T3-L1 cells. Exposure to 10 μM Forskolin for 20 minutes disrupted the arrangement of F-actin filaments but with some intact filaments still observed, whereas exposure to 10 μM cytochalasin D has segmented the actin filaments. The cytochalasin-induced F-actin segmentation we observed is similar to the effect of cytochalasin D that has been reported previously to inhibit the polymerisation of the actin cytoskeleton, which leads to major effects on cell stiffness, motility, and contraction (28). It has been known for some time that cytochalasin-D inhibited the serum-induced contraction of collagen gels in which rat mesangial cells were embedded (29). The disruption of the F-actin cytoskeleton by cytochalasin-D resulted in a dramatic reduction in the traction forces of alveolar epithelial cells that are induced by thrombin (30). Forskolin activates adenylyl cyclase and leads to an increase in cytosolic cAMP concentration (31). It has been shown that an increase in the cytosolic cAMP concentration in T lymphocytes is associated with a decrease in the amount of F-actin expressed by the cell (32). Increasing the intracellular cAMP concentration using forskolin reduced by 30% the contractile force of retinal epithelial cells embedded in collagen gel (33). Forskolin has also been shown to disrupt the assembly of actin stress fibres and focal adhesion complexes in fibroblasts, most likely through intracellular pathways that elevate cAMP and incrase protein kinase 1 activity (34).

We measured that forskolin caused less relaxation of the capsules (3% deformation) compared to cytochalasin-D (7%). We have previously observed the density of 3T3-LI cell growth on polyelectroyte films to be approximately 395 cells per mm2 (16). The surface area of the PAH-starting polyelectrolyte capsules was 15.4 mm2, which meant that each capsule had approximately 6,083 cells growing on its surface. From our measurements of the force associated with either forskolin or cytochalasin-D, we can calculate that the force associated with the forskolin-induced relaxation of a single cell is 3.2 nN and the force associated with the cytochalasin-D-induced relaxation of a single cell is 7.5 nN. These forces are within the range of 0.1nN to 50nN reported in the literature (35, 36, 37, 38).

Conclusion

We describe a simple assay for cell contractility that is based on the deformation of a hollow deformable capsule. We measured the contraction force using compounds to disrupt the F-actin cytoskeleton and thus to induce a relaxation of the capsules that were previously contracted by the cells. The mechanism of action of forskolin through second messenger pathways to disrupt the assembly of actin stress fibres also explains its reduced effect on cell contraction compared to that for cytochalasin-D, which is a compound that directly inhibits the polymerization of F-actin filaments.

Conflict of Interest

The authors declare no financial or commercial conflict of interest.

References

1. Harris A, Wild P, Stopak D. Silicone rubber substrata: A new wrinkle in the study of cell locomotion. Science, 1980; 208:177-179
2. Markhotina N, Liu GJ, Martin DK. Contractility of retinal pericytes grown on silicone elastomer substrates is through a protein kinase A-mediated intracellular pathway in response to vasoactive peptides. IET Nanobiotechnol, 2007; 1:44-51
3. du Roure O, Saez A, Buguin A, Austin RH, Chavrier P, Silberzan P, Ladoux B. Force mapping in epithelial cell migration. Proc Natl Acad Sci USA, 2005; 102:2390-2395
4. Park J, Ryu J, Choi SK, Seo E, Cha JM, Ryu S, Kim J, Kim B-S, Lee SH. Real-time measurement of the contractile forces of self-organized cardiomyocytes on hybrid biopolymer microcantilevers. Anal Chem, 2005; 77:6571-6580
5. Kelley C, D'Amore P, Hechtman H, Shepro D. 1987, Microvascular pericyte contractility *in vitro*: Comparison with other cells of the vascular wall. J Cell Biol, 1987; 104:483-490
6. Elsdale T, Bard J. Collagen substrata for studies on cell behaviour. J Cell Biol, 1972; 54:626-637
7. Buttafoco L, Boks N, Engubers-Buijtenhuijs P, Grijpma DW, Poot A, Dijkstra P, Vermes I, Feijen J. Porous hybrid structures based on P(Dlla-Co-Tmc) and collagen for tissue engineering of small diameter blood vessels. J Biomed Mater Res B, 2006; 79:425-434
8. He W, Ma Z, Yong T, Teo WE, Ramakrishna S. 2005, Fabrication of collagen-coated biodegradable polymer nanofiber mesh and its potential for endothelial cells growth. Biomaterials, 2005; 36:7606-7615
9. Yang J, Motlagh D, Webb AR, Ameer GA. Novel biphasic elastomeric scaffold for small-diameter blood vessel tissue engineering. Tissue Eng, 2005; 11:1876-1886
10. Amiel GE, Komura M, Shapira O, Yoo JJ, Yazdani S, Berry J, Kaushal S, Bischoff J, Atala A, Soker S. 2006, Engineering of blood vessels from acellular collagen matrices coated with human endothelial cells. Tissue Eng, 2006; 12:2355
11. Takei T, Yamaguchi S, Sakai S, Ijima H, Kawakami K. Novel technique for fabricating double-layered tubular constructs consisting of two vascular cell types in collagen gels used as templates for three-dimensional tissues. J Biosci Bioeng, 2007; 104:435-438
12. Decher G. Fuzzy nanoassemblies: Toward layered polymeric multicomposites. Science, 1997; 277:1232-1237
13. Georgieva R, Moya S, Donath E, Baumler H. Permeability and conductivity of red blood cell templated polyelectro-

lyte capsules coated with supplementary layers. Langmuir, 2004; 20:1895-1900
14. Vautier D, Karsten V, Egles C, Chluba J, Schaaf P, Voegel JC, Ogier J. Polyelectrolyte multilayer films modulate cytoskeletal organization in chondrosarcoma cells. J Biomater Sci Polym Ed, 2002; 13:712-731
15. Boura C, Menu P, Payan E, Picart C, Voegel JC, Muller S, Stoltz JF. Endothelial cells grown on thin polyelectrolyte mutlilayered films: An evaluation of a new versatile surface modification. Biomaterials, 2003; 24:3521-3530
16. Ting JHY, Haas MR, Valenzuela SM, Martin DK. Terminating polyelectrolyte in multilayer films influences growth and morphology of adhering cells. IET Nanobiotechnol, 2007; 4:77-90
17. Battle A, Valenzuela SM, Mechler A, Nichols RJ, Praporski S, di Maio, Isalm H, Girard-Egrot AP, Cornell BA, Prashar J, Caruso F, Martin LL, Martin DK. Novel engineered ion channels provides controllable ion permeability for polyeletrolyte microcapsules with a lipid membrane. Advanced Functional Materials, 2009; 19:201-208
18. Stidder B, Alcaraz JP, Liguoori L, Khalef N, Bakri A, Watkins EB, Cinquin P, Martin DK. Biomimetic membrane system composed of a composite interpenetrating hydrogel film and a lipid bilayer. Advanced Functional Materials, 2012; 22:4259-4267
19. Petra Tryoen-Tóth DV, Haikel Y, Voegel JC, Schaaf P, Chluba J, Ogier J. Viability, adhesion, and bone phenotype of osteoblast-like cells on polyelectrolyte multilayer films. J Biomed Mater Res, 2002; 60:657-667
20. Lin Y, Wang L, Zhang P, Wang X, Chen X, Jing X, Su Z. Surface modification of poly(L-Lactic Acid) to improve its cytocompatibility via assembly of polyelectrolytes and gelatin. Acta Biomater, 2006; 2:155-164
21. Mermut O, Lefebvre J, Gray D, Barrett C. Structural and mechanical properties of polyelectrolyte multilayer films studied by AFM. Macromolecules, 2003; 36:8819-8824
22. Heuvingh J, Zappa M, Fery A. Salt softening of polyelectrolyte multilayer capsules. Langmuir, 2005; 21:3165-3171
23. Lulevich V, Andrienko D, Vinogradova O. Elasticity of polyelectrolyte multilayer microcapsules. J Chem Phys, 2004; 120:3822-3826
24. Antipov AA, Sukhorukov G.B. Polyelectrolyte multilayer capsules as vehicles with tunable permeability, Advances in Colloid and Interface Science Plenary and Invited Lectures From the XVIth European Chemistry at Interfaces Conference, Vladimir, Russia, May 2003, vol. 111, no. 1-2, pp. 49-61
25. Antipov AA, Shchukin D, Fedutik Y, Petrov AI, Sukhorukov GB, Möhwald H. Carbonate microparticles for hollow polyelectrolyte capsules fabrication. Coll Surf A, 2003; 224:175-183
26. Lebedeva OV, Kim BS, Vasilev K, Vinogradova OI. Salt softening of polyelectrolyte multilayer microcapsules. J Coll Interf Sci, 2005; 284:455-462
27. Obara K, Nikcevic G, Pestic L, Nowak G, Lorimer DD, Guerriero V Jr, Elson EL, Paul RJ, Lanerolle PD. Fibroblast contractility without an increase in basal myosin light chain phosphorylation in wild type cells and cells expressing the catalytic domain of myosin light chain kinase. J Biol Chem, 1995; 270:18734-18737
28. Wakatsuki T, Schwab B, Thompson NC, Elson EL. Effects of cytochalasin D and larunculin B on mechanical properties of cells. J Cell Sci, 2001; 114:1025-1036
29. Allenberg M, Weinstein T, Li I, Silverman M. Activation of procollagenase IV by cytochalasin D and concanavalin A in cultured rat mesangial cells: linkage to cytoskeletal reorganization. J Amer Soc Nephrol, 1994; 4:1760-1770
30. Gavara N, Sunyer R, Roca-Cusachs P, Farré R, Rotger M, Navajas D. Thrombin-induced contraction in alveolar epithelial cells probed by traction microscopy. J Appl Physiol, 2006; 101:512-520
31. Insel PA, Ostrom RS. Forskolin as a tool for examining adenylyl cyclase expression, regulation and G-protein signaling. Cell Molec Neurobiol, 2003; 23:305-314
32. Valitutti S, Dessing M, Lanzavecchia A. Role of cAMP in regulating cytoxic T lymphocyte adhesion and motility. Eur J Immunol, 1993; 23:790-795
33. Smith-Thomas LC, Richardson PSR, Rennie IG, Palmer I, Boulton M, Sheridan C, MacNeil S. Influence of pigment content, intracellular calcium and cyclicAMP on the ability of retinal pigmen,t epithelial cells to contract collagen gels. Curr Eye Res, 2000; 21:518-529
34. Swaney JS, Patel HH, Yokoyama U, Head BP, Roth DM, Insel PA. Focal adhesions in (myo)fibroblasts scaffold adenylyl cyclase with phosphorylated caveolin. J Biol Chem, 2006; 281:17173-17179
35. Freyman TM, Yannas IV, Yokoo R, Gibson LJ. Fibroblast contraction of a collagen-gag matrix. Biomaterials, 2001; 22:2883-2891
36. Eastwood M, McGrouther DA, Brown RA. A culture force monitor for measurement of contraction forces generated in human dermal fibroblast cultures: evidence for cell-matrix mechanical signalling. Biochim Biophys Acta, 1994; 1201:186-192
37. Delvoye P, Wiliquet P, Leveque JL, Nusgens BV, Lapiere CM. Measurement of mechanical forces generated by skin fibroblasts embedded in a three-dimensional collagen gel. 1991; 97:898-902
38. Kasugai S, Suzuki S, Shibata S, Yasui S, Amano H, Ogura H. 1990, Measurements of the isometric contractile forces generated by dog periodontal ligament fibroblasts *in vitro*. Arch Oral Biol, 1990; 35:597-601